Injection Molding of a Starch/EVOH Blend Aimed as an Alternative Biomaterial for Temporary Applications

RUI A. SOUSA,[1,2] GÜRHAN KALAY,[1] RUI L. REIS,[2] ANTÓNIO M. CUNHA,[2] MICHAEL J. BEVIS[1]

[1] Wolfson Centre for Materials Processing, Brunel University, Uxbridge, Middlesex, UB8 3PH, United Kingdom

[2] Department of Polymer Engineering, University of Minho, Campus de Azurém, 4800 Guimarães, Portugal

Received 15 July 1999; accepted 26 December 1999

ABSTRACT: Biodegradable polymers show great potential to be used as materials for temporary implants and bone replacement applications in orthopedics. However, its use in high load-bearing applications will depend on the successful development of biodegradable implants with a mechanical performance matching that of human bone. This article describes the optimization of the injection molding process of an alternative biodegradable starch-based polymer aimed at biomedical applications. A blend of starch with a copolymer of ethylene–vinyl alcohol (SEVA-C) was studied. Both conventional injection molding and shear controlled orientation (SCORIM) were optimized with the support of design of experiments and analysis of variance techniques. The mechanical characterization was performed by tensile testing. The structure developed within the moldings was assessed by wide-angle X-ray diffraction and differential scanning calorimetry. Increases up to 30% in the tangent modulus and 20% in the ultimate tensile strength compared with conventional molding were achieved with the application of SCORIM. The holding pressure and the frequency of the shear applied have the strongest influence on the morphology development and consequently on the mechanical performance. The solidification of SEVA-C at high cavity pressures enhances stiffness for long durations of the shearing stage in SCORIM. However, the effect of viscous heating of SEVA-C is important and ought to be considered. A decrease of the material phase miscibility in SEVA-C occurs as result of the shear fields imposed. The microstructure evaluation suggests that the mechanical properties enhancement in SCORIM molded SEVA-C is attributable to preferred orientation developed during processing. © 2000 John Wiley & Sons, Inc. J Appl Polym Sci 77: 1303–1315, 2000

Key words: starch; biodegradable; biomaterial; injection molding; SCORIM; design of experiments

INTRODUCTION

Polymer-based composites are found in clinical applications more extensively now than in the past.[1–3] Orthopedics is one of the main areas of potential use for these composites,[4–6] where it is essential to achieve a mechanical performance of the implant as close as possible to that of human bone, to avoid clinical problems related to the mechanical mismatch between the bone and the surgical implant.[7,8] In fact, the use of very stiff materials leads to stress protection of the healing bone, i.e., resulting in osteoporosis phenomena due to the absence of normal functional loading.[8] Biodegradable polymers are a promising alterna-

Correspondence to: G. Kalay (Gurhan.Kalay@brunel.ac.uk).

Contract grant sponsor: Subprograma Ciência e Tecnologia do 2° Quadro Comunitário de Apoio, Ministério da Ciência e Tecnologia, Portugal (to R.A.S.).

Journal of Applied Polymer Science, Vol. 77, 1303–1315 (2000)

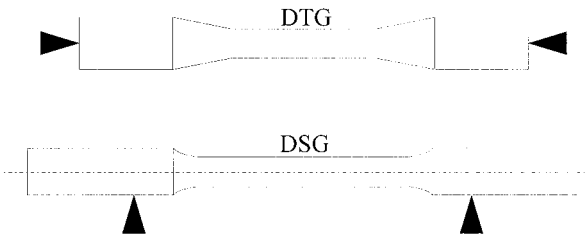

Figure 1 Schematic diagram of the DSG and DTG moldings (black arrows indicate gating points).

tive for implants, because as they degrade in the body, a second surgery for implant removal may be avoided. Furthermore, biodegradable implants also may enable a dynamic process of bone healing, allowing a gradual stress transfer to the tissue.[6–8]

The high stiffness of human cortical bone arises from the properties and structural arrangements of its phases, i.e., collagen and hydroxylapatite.[9] The mechanical character results from the preferred alignment of the hydroxylapatite lamellae and of the collagen chains that occur at different structural levels.[9–12] The reproduction of this complex morphology, although challenging, is expected to be a successful route for the development of load-bearing surgical implants that do not lead to stress protection of the bone. So the route for the development of hard tissue replacement should mimic the bone morphology as well as its chemistry to achieve not only the mechanical specifications but also to assure the adequate interactions with living tissues.

Despite several advantages for temporary bone fixation, the use of biodegradable polymers is still limited to low load-bearing applications. Degradable polymer-based composites with improved mechanical performance have been obtained by self-reinforcement of matrix materials such as polylactic acid[5,6] or polyglicolic acid[5,6] and using specific ceramics as reinforcements.[3,6,7] Corn starch-based blends[13–15] were proposed as an alternative to the referred systems, namely a blend of native corn starch with poly(ethylene vinyl alcohol) (SEVA). These materials exhibit a thermoplastic behavior and degrade in the presence of body simulated fluids.[16,17] The bioactive character is assured by the use of an inorganic filler, hydroxylapatite, that also acts as mechanical reinforcement.

Following previous results, the approach used is based on the combination of a biodegradable system and bioactive reinforcement and a deliberately induced morphology during the respective processing operation, by means of shear controlled orientation in injection molding polymer (SCORIM). In this molding technique, the polymer solidification takes place under a controlled macroscopic shear field that induces orientation of the molecular structure.[18,19] The influence of SCORIM processing on the final morphology of injection-molded polymers and polymer-based composites were discussed elsewhere.[20–24] It was shown that a simultaneous increase both in stiffness and impact strength is possible for various thermoplastics.[23–26]

The use of nonconventional processing techniques on SEVA and SEVA/hydroxylapatite composites was also studied by Reis et al.,[27,28] who reported an enhancement of the mechanical properties. In fact, the combined use of twin-screw extrusion in the compounding stage and of SCORIM in the molding process allowed for the development of starch-based composites with an induced structural orientation and superior me-

Table I Processing Conditions for the Conventional Moldings (CM) of SEVA-C

	CM-S	CM-T
Injection pressure[a] (MPa)	11.3	11.3
Holding pressure[a] (MPa)	5.0	5.0
Injection time (s)	0.5	5.0
Holding pressure time (s)	20.0	14.0
Cooling time (s)	10.0	20.0
Cycle time (s)	31.5	40.0
Mold temperature (°C)	60	40
Melt Temperature (°C)	170	170

[a] Pressures in the machine's hydraulic system

Table II Levels of the Processing Parameters for SCORIM DSG Moldings of SEVA-C, Arrays 1 and 2

	Low	High
Array 1		
Holding pressure[a] (MPa)	1.3	2.6
Frequency of piston movements[b] (Hz)	0.50	1.00
Array 2		
Holding pressure[a] (MPa)	2.6	3.9
Duration of shear applied (stage S2) (s)	12.0	24.0

[a] Pressures in the machine's hydraulic system.
[b] For each one of the consecutive SCORIM stages (S0, S1, S2).

Table III Processing Conditions for SCORIM DSG Moldings of SEVA-C

	Array 1	Array 2
Injection pressure[a] (MPa)	11.3	11.3
Holding pressure[a] (MPa)	—	—
Injection time (s)	1.5	1.5
Holding pressure time (s)	37.0	—
Cooling time (s)	20.0	20.0
Cycle time (s)	59.5	—
Mold temperature (°C)	60	60
Melt Temperature (°C)	170	170
Number of SCORIM stages	3	3
Stage duration[b] (s)	1, 12, 24	1, 12, —
Frequency of piston movements[b] (Hz)	1.00, —, —	1.00, 1.00, 1.00
Piston pressures[b] (%)	31, 30, 28	31, 30, 28

[a] Pressures in the machine's hydraulic system.
[b] For each one of the consecutive SCORIM stages (S0, S1, S2).

chanical properties. Biodegradable composites with modulus above 7 GPa were produced and a possibility for further improvement is envisaged.[29]

The present study was developed to quantify the influence of SCORIM processing parameters on the mechanical properties of nonreinforced SEVA. It envisages the optimization of the respective processing setup and the identification of the determinant parameters.

MATERIALS AND METHODS

Material

The study material was a blend of starch and a copolymer of poly(ethylene-vinyl alcohol) 60:40 (mol/mol) (SEVA-C), grade Mater-Bi 1128 RR, supplied by Novamont, Novara, Italy, with a melt flow index value of 0.71 g/10 min (170°C, 49*N*).

Injection Molding

A Demag D-150 NCIII-K conventional injection molding machine fitted with a SCORIM head was used to produce cylindrical tensile test samples with 5-mm diameter. Two mold geometries were produced: 1. tensile test bar with 36-mm gauge length and with a double side gating system; and 2. tensile test bar with 25-mm gauge length and with a double top gating system. These tensile test bars were named respectively as DSG and DTG (a schematic diagram of these moldings is

Table IV Processing Conditions for the SCORIM DTG Moldings of SEVA-C

	SCA-T/SCB-T SCC-T	SCE-T/SCF-T SCG-T	SCH-T/SCI-T SCJ-T
Injection pressure[a] (MPa)	11.3	11.3	11.3
Holding pressure[a] (MPa)	7.6	5.0	7.6
Injection time (s)	1.5	1.5	1.5
Holding pressure time (s)	14.0	14.0	14.0
Cooling time (s)	20.0	20.0	20.0
Cycle time (s)	36.5	36.5	36.5
Mold temperature (°C)	40	40	40
Melt Temperature (°C)	170	170	170
Number of SCORIM stages	2	2	2
Stage time[b] (s)	2, 12	2, 12	2, 12
Frequency of piston movements[b] (Hz)	1.0, (1.00/0.50/0.33)	1.0, (1.00/0.50/0.33)	1.0, (1.00/0.50/0.33)
Piston pressures[b] (%)	41, 40	41, 40	51, 50

[a] Pressures in the machine's hydraulic system.
[b] For each one of the consecutive SCORIM stages (S0, S1).

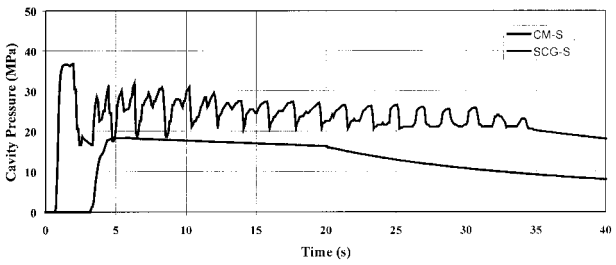

Figure 2 Cavity pressure profiles for CM-S and SCG-S.

shown in Figure 1). Two molding techniques were used: 1. conventional injection molding; and 2. shear controlled orientation injection molding. Several processing parameters were studied in SCORIM processing following a design of experiments plan. The parameters considered were the holding pressure, the piston pressures (packing and relaxation), the frequency of piston movements, and the duration of shear applied. The SCORIM setup was based on two or three stages (respectively for DTG and DSG molding geometry) and on mode A operation (out of phase operation of the oscillating hydraulic pistons).[23] The consecutive SCORIM stages were designated sequentially as S0, S1, and S2. The duration of the shear action of the pistons and the respective frequency and pressure were defined for each SCORIM stage. The cavity pressure profile was monitored by piezo-electric transducer measurements, to control any variation during processing and to evaluate the influence of the different processing conditions applied in molding.

One conventional injection-molding batch was produced for each mold geometry. Conventional moldings for DSG and DTG geometries will be referred respectively as CM-S and CM-T. The processing conditions used for conventional moldings of SEVA-C are summarized in Table I.

The processing conditions for the DSG SCORIM moldings were defined according to a design of experiments based in two L4 arrays (Table II). This specific design for DSG moldings was chosen according to the high susceptibility of SEVA-C to thermo-mechanical degradation (induced by the viscous dissipation associated with the high shear stresses imposed during processing) and the narrow processing window. In the first array, the studied parameters were the holding pressure and the frequency of piston movements. Four injection molding sets were produced and described as follows:

1. SCA-S at low holding pressure and low frequency of piston movements.
2. SCB-S at low holding pressure and high frequency of piston movements.
3. SCC-S at high holding pressure and low frequency of piston movements.
4. SCD-S at high holding pressure and high frequency of piston movements.

The processing parameters studied in the second array were the holding pressure and the duration of piston movements, by means of the duration of stage S2. Four sets of moldings were produced, namely:

1. SCE-S at low holding pressure and short duration of piston movements.
2. SCD-S at low holding pressure and long duration of piston movements.
3. SCF-S at high holding pressure and short duration of piston movements.
4. SCG-S at high holding pressure and long duration of piston movements.

Note that SCD-S is common to both arrays. The frequencies of piston movements presented in Tables II, III, and IV are defined according to the compression and relaxation times of the SCORIM pistons. The values of piston pressures shown for each SCORIM molding are referred as percentage of the machine's maximum capacity. Table III summarizes the processing conditions for the DSG moldings. The cavity pressure profile for SCG-S is shown in Figure 2 together with a typical cavity pressure profile for CM-S.

No specific experimental design was used for DTG moldings. For each variation of the studied parameters, equally spaced intervals were selected. Shorter cycle times, as compared with DSG moldings, were used to minimize the residence time and to avoid thermal degradation of

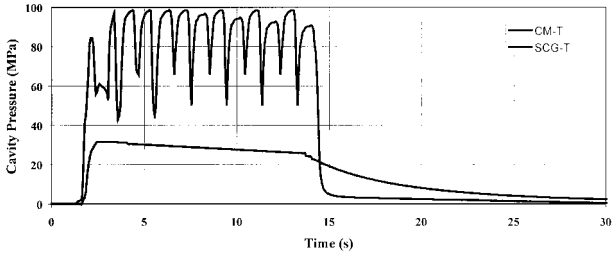

Figure 3 Cavity pressure profiles for CM-T and SCG-T.

Table V Best Tensile Test Results for Both Conventional and SCORIM Moldings of SEVA-C

Set	Tangent Modulus (MPa)	Secant Modulus (MPa)	Ultimate Tensile Strength (MPa)	Strain at Peak (%)	Strain at Break (%)
CM-S	2275 (118)	2061 (97)	41.0 (1.8)	1.6 (0.45)	7.1 (5.2)
SC0C-S	2555 (104)	2278 (71)	46.4 (1.5)	3.2 (0.66)	12.8 (2.6)
SC0D-S	2505 (183)	2257 (171)	44.9 (2.3)	2.0 (0.52)	7.4 (4.7)
SCE-S	2601 (153)	2351 (144)	48.0 (2.0)	2.4 (0.23)	22.4 (8.5)
SCG-S	2972 (205)	2624 (172)	48.9 (2.2)	1.9 (0.07)	11.1 (3.8)
CM-T	2166 (130)	1955 (94)	42.6 (0.9)	2.5 (0.06)	20.0 (4.5)
SCF-T	2719 (201)	2435 (164)	49.2 (1.0)	2.5 (0.22)	9.5 (3.0)
SCG-T	2615 (159)	2342 (144)	51.7 (2.0)	2.5 (0.18)	12.3 (2.5)

Standard deviations are shown in parenthesis.

the material. The influence of frequency of piston movements was studied in nine sets, which may be briefly described as follows:

1. SCA-T, SCB-T, and SCC-T at high, medium, and low frequencies of piston movements respectively, at high holding pressure and medium piston pressures.
2. SCD-T, SCE-T, and SCF-T at high, medium, and low frequencies of piston movements respectively, at low holding pressure and medium piston pressures.
3. SCG-T, SCH-T, and SCI-T at high, medium, and low frequencies of piston movements respectively, at high holding and piston pressures.

Table IV summarizes the processing conditions for these sets. Melt temperatures of 170°C (temperature profile in the barrel: 170/170/160/150/140°C) were used for all the SEVA-C moldings. The cavity pressure profiles for CM-T and SCG-T are shown in Figure 3.

Tensile Testing

The tensile tests were performed on an Instron 4505 universal testing machine fitted with an Instron 2630 resistive extensometer with 10-mm gauge length. The tensile test bars were tested to determine the tangent modulus, the secant modulus at 0.8% strain, the ultimate tensile strength, the strain at peak, and the strain at break. The tests were performed in a controlled environment (23°C and 55% RH) with a cross-head speed of 5 mm/min (8.3×10^{-5} m/s) until 1.5% strain, to determine accurately the modulus, and then increased to 50 mm/min (8.3×10^{-4} m/s) until rupture.

Wide Angle X-ray Diffraction (WAXD) and Debye Patterns

Cu K_α radiation was used to obtain X-ray diffraction spectra and Debye patterns. These patterns were used to assess the preferred orientation of the moldings. The diffraction data were obtained at a scanning rate of 0.02° 2θ/s and over a Brag

Table VI Analysis of Variance for the Tangent Modulus for Array 1 of SEVA-C

Source of Variation	SS	df	V	*F*
Main effects				
Frequency of piston movements	56,498	1	56,498	2.9
Holding pressure	415,008	1	415,008	21.3
Two factors interaction				
Frequency of piston movements; holding pressure	120,901	1	120,901	6.2
Residual	311,010	16	19,438	
Total	903,418	19		

Table VII Analysis of Variance for the Tangent Modulus for Array 2

Source of Variation	SS	df	V	*F*
Main effects				
Duration of shear applied	220,710	1	220,710	7.8
Holding pressure	129,122	1	129,122	4.6
Two factors interaction				
Duration of shear applied; holding pressure	468,486	1	468,486	16.6
Residual	450,824	16	28,176	
Total	1,269,143	19		

angle range of $0° < 2\theta < 50°$. The samples were cut parallel to the flow direction with a thickness of 1 mm. The Debye patterns were obtained at positions of 1.5 mm from the edge of the moldings. An aperture of 100 μm diameter was used to define the position and cross section of the incident X-ray beam.

Differential Scanning Calorimetry (DSC)

Calorimetric studies were performed on a differential scanning calorimeter Perkin Elmer DSC 7, to assess the crystallinity of moldings produced by the different processing routes used. Each sample was cut from the middle point of the gauge length of the tensile test bars, with an average weight between 7 and 9 mg. The samples were placed in aluminum pans and heated at a rate of 10.0°C per min (0.16°C/s) from 30 to 180°C.

Scanning Electron Microscopy (SEM)

SEM was used for fractographic analysis and was performed on selected sets on a Leica Cambridge scanning electron microscope. All the surfaces were mounted on a copper stub and coated with Au/Pd alloy before examination.

Statistical Analysis

Analysis of variance (ANOVA) was applied to the tensile test results according to each design of experiments described. A two-way ANOVA was performed for L4 arrays in DSG moldings to evaluate the effects of the parameters. One-way analysis was also used to evaluate the isolated effect of a processing parameter on the total variation. For all cases, an *F* test, at 95% confidence level, was applied to quantify the significance between samples' averages. Tables VI to IX summarize the ANOVA results, where the total sums of squares is the measure of the total variation present in the data collected for one specific experimental design. In the one-way ANOVA, this measure can be decomposed into several sources: a variation due to a controlled parameter (main effect) and a variation due to an error (residual). In two-way ANOVA, the total variation is also composed of two additional sources of variation: a variation due to a second controlled parameter (main effect) and a variation due to the interaction between controlled parameters (two factor interaction). The total degrees of freedom are related to the number of independent comparisons able to be made with the data. For each case, the degrees of

Table VIII Analysis of Variance for the Tangent Modulus for SCA-T to SCG-T

Source of Variation	SS	df	V	*F*
Main effects				
Frequency of piston movements	1,158,965	2	579,483	25.1
Holding pressure	75,802	1	75,802	3.3
Two factors interaction				
Frequency of piston movements; holding pressure	373,005	2	186,503	8.1
Residual	553,028	24	23,043	
Total	2,160,801	29		

Table IX Analysis of Variance for the Ultimate Tensile Strength for SCA-T to SCF-T

Source of Variation	SS	df	V	*F*
Main effects				
Frequency of piston movements	83.3	2	41.6	20.2
Holding pressure	76.2	1	76.2	36.9
Two factors interaction				
Frequency of piston movements; holding pressure	11.5	2	5.8	2.8
Residual	49.5	24	2.1	
Total	220.5	29		

freedom are defined according to the experimental design used and can be decomposed into several sources. Considering the two-way ANOVA example, the total degrees of freedom is given by the sum of degrees of freedom associated with: the first controlled parameter, the second controlled parameter, the interaction between controlled parameters and the error. The variance (V) is given by the quotient of each sum of squares by the respective degrees of freedom. The error variance (or the residual variance) is a measure of the variation due to uncontrolled factors. The *F* test consists of the ratio of two estimates of the individual variance: a variance due to a main effect (or interaction) and a variance due to an error. The significance of this quotient is determined by the degrees of freedom of the numerator, the denominator, and by the confidence level desired. Parameters or interactions that present an *F* ratio larger than a defined criterion will be considered relevant and are believed to influence the average value of the population. Detailed description of the mathematical fundamentals of ANOVA as well as of other statistical analyses, suitable to experimental interpretation of data, can be found elsewhere.[30–32]

Data obtained according to experimental designs with more than four experimental points were fitted to a third order polynomial equation. For each case, the polynomial equation was chosen according to a goodness of fit criteria based on *F*-statistics.[32] A three-dimensional surface was generated and used to describe the dependence of mechanical performance on processing parameters. Figures 9 to 11 show such dependence according to the surface fitting described.

RESULTS AND DISCUSSION

Tensile Testing and Statistical Analysis

The best tensile test results for DSG and DTG moldings are summarized in Table V for CM-S, SCC-S, SCD-S, SCE-S, SCG-S, CM-T, SCF-T, and SCG-T. The DSG conventional moldings exhibit a tangent modulus of 2275 MPa, an ultimate tensile strength of 41.0 MPa and a strain at peak of 1.6%. A comparison with SCG-S moldings shows an increase of 31% in tangent modulus and 19% in UTS, following the application of SCORIM. Also an increase in tangent modulus and in UTS of, respectively, 14 and 17% were achieved for SCE-S molded with a shorter duration of shear applied. The DTG conventional moldings (CM-T) exhibit a tangent modulus of 2166 MPa, an ultimate tensile strength of 42.6 MPa, and a strain at peak of 2.5%. These values represent increases of 25 and 15%, respectively, for tangent modulus and UTS, by means of the use of SCORIM in SCF-T moldings. Figure 4 shows the tensile failure surface of CM-S, exhibiting a planar fracture surface which is consistent with the mechanical behavior exhibited by the sample. Figure 5 shows the tensile failure surface for SCG-S, featuring a highly orientated structure and shows a distinct skin/core morphology as a result of the shear loads applied during molding. The stress-strain diagrams for CM-S and SCG-S are presented in Figure 6.

A maximum increase in tangent modulus of 12% relative to conventional molding was achieved for SCC-S in array 1. Figure 7 shows the variation of the tangent modulus in this array for two levels of the holding pressure and frequency of piston movements, showing an overall positive dependence on these variables. Considering the degrees of freedom involved, a processing parameter (or interaction) will be considered relevant (for a confidence level of 95%) if its *F* value, presented by ANOVA analysis, is larger than 4.5.[30] According to the ANOVA results presented in Table VI, the holding pressure (with an *F* value of 21.3) is the only significant parameter. The fre-

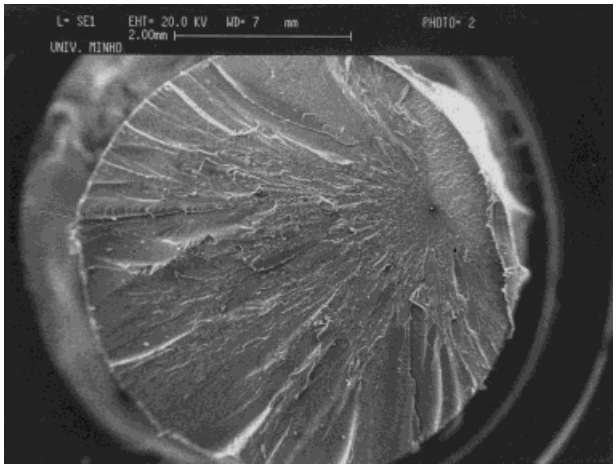

Figure 4 Typical tensile fracture surface of CM-S moldings.

quency of piston movements is believed to have no effect on the average of the population analyzed.

In array 1 an improvement of 17% is also achieved in the ultimate tensile strength for SCB-S (compared with conventional molding). In this case, the frequency of piston movements presents an F value of 19.9 and is the most important processing parameter. The interaction between processing parameters is the main source of variation resulting in an F value of 39.7. Both results show the interdependence of processing parameters in SCORIM processing. The final properties of moldings are determined simultaneously by holding pressure and by frequency of piston movements. In fact, it is evident from this analysis that enhancement of stiffness in SEVA moldings is favored by solidification of the polymer at high cavity pressures.

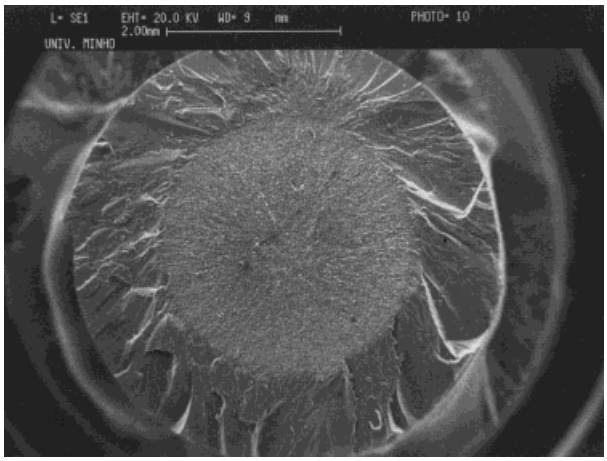

Figure 5 Typical tensile fracture surface of SCG-S moldings.

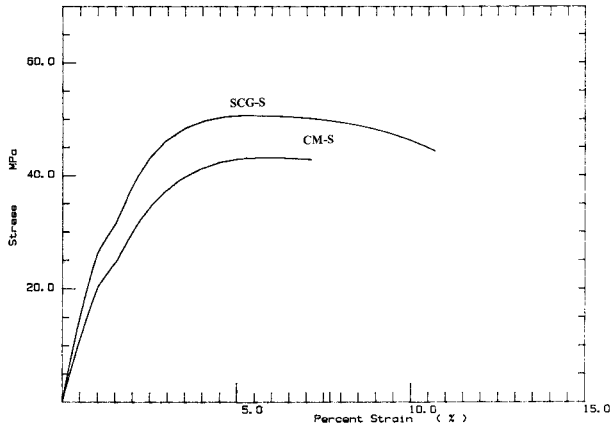

Figure 6 Stress-strain curves for CM-S and SCG-S.

Figure 8 shows the variation of the tangent modulus for two levels of the holding pressure and duration of shear applied for array 2. The maximum value is achieved in SCG-S for higher holding pressures and longer durations of shear applied. The results of ANOVA, presented in Table VII, show that the duration of shear applied is the most important main effect with an F value of 7.8. The larger source of variation is the interaction of the processing parameters with an F value of 16.2. Once again SEVA stiffness is favored by the combination of high holding pressures with long periods of shear. However, the susceptibility

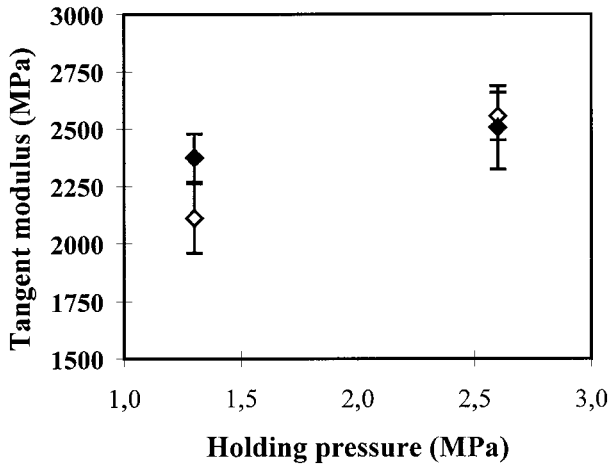

Figure 7 Tangent modulus variation for SEVA-C for two levels of the holding pressure and frequency of piston movements: ♦, 1.00 Hz of frequency of piston movements; ◇, 0.50 Hz of frequency of piston movements.

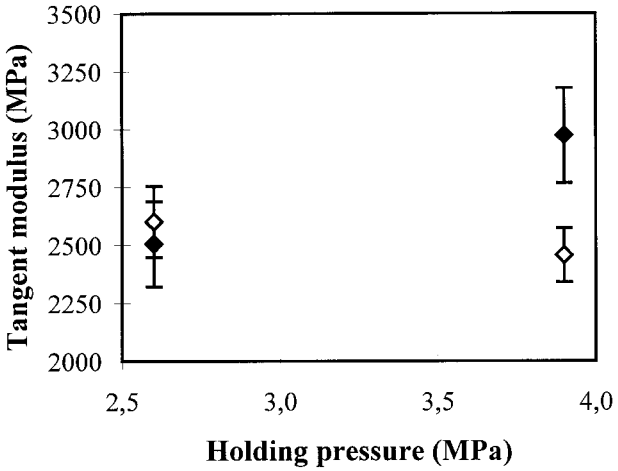

Figure 8 Tangent modulus variation for SEVA-C for two levels of the holding pressure and duration of shear applied in SCORIM stage S2: ◇, 12 s of duration of shear applied; ♦, 24 s of duration of shear applied.

to thermal degradation should be considered during the processing setup. A high level of holding pressure leads to pronounced viscous heating and reduces the safe residence time, thereby causing severe thermal degradation of the polymer when a long duration of shear is applied.

The tangent modulus is surface plotted for SCA-T to SCF-T as a function of frequency of piston movements and holding pressure in Figure 9. At both holding pressures, a maximum occurs for low frequency of piston movements. In this design, a source of variation will be considered relevant for a confidence level of 95%, if its F value is higher than 3.4. The ANOVA results presented in Table VIII, show that the greatest effect is the frequency of piston movements with an F value of 25.1. The interaction of the processing parameters is the second largest source of variation with an F value of 8.1. The enhancement of stiffness is favored by lower frequencies of piston movements.

Figure 10 shows the variation of the ultimate tensile strength for SCA-T to SCF-T. An improvement in ultimate tensile strength of 15% is achieved in SCF-T (compared with conventional moldings). The greatest effect on the variation of the ultimate tensile strength is the holding pressure with an F value of 36.9 (Table IX). The frequency of piston movements presents an F value of 20.2.

The variation of the tangent modulus as a function of the frequency of piston movements and piston pressures for SCA-T to SCC-T and for

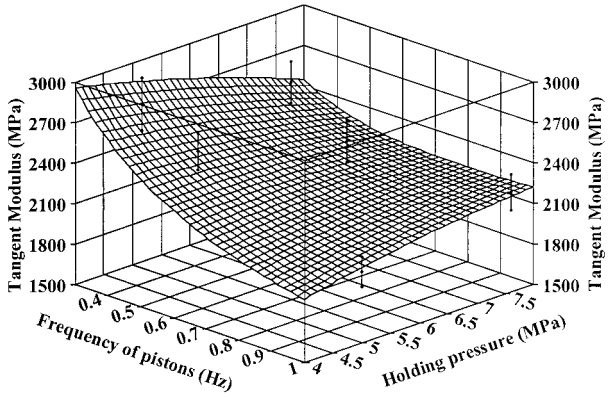

Figure 9 Tangent modulus variation for SEVA-C as a function of frequency of piston movements and holding pressure.

SCG-T to SCI-T is plotted in Figure 11. An improvement of 27% in tangent modulus is achieved in SCI-T, molded at high piston pressures and medium frequency of piston movements. The piston pressures present an F value of 6.05 and is the largest main effect. The interaction of the processing parameters is the most important source of variation with an F value of 22.1. For each pair of holding/piston pressures exists a frequency of piston movements for which the development of an oriented morphology is maximum.

Wide Angle X-ray Diffraction and Debye Patterns

Figure 12 shows the diffraction profiles for CM-S, SCC-S, and SCG-S. An increase in the crystalline peak area occurs following the application of SCORIM. A peak at 2θ of 10.89 and d-spacing of

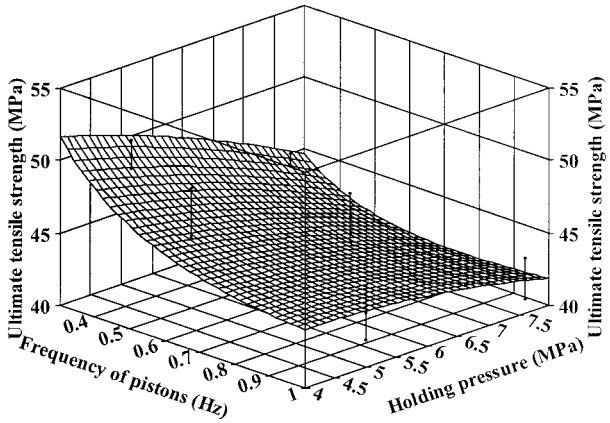

Figure 10 Ultimate tensile strength variation for SEVA-C as a function of frequency of piston movements and holding pressure.

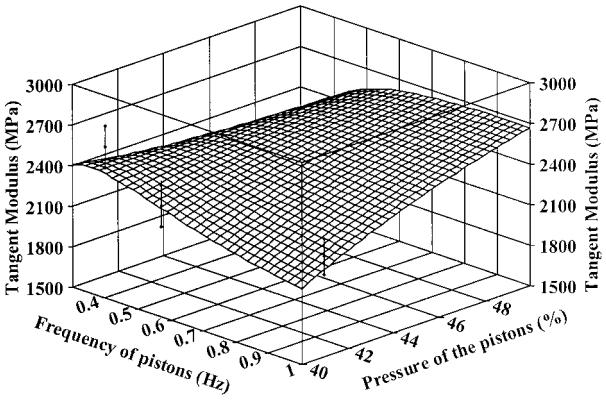

Figure 11 Tangent modulus variation for SEVA-C as a function of frequency of piston movements and average piston pressures.

8.128 Å is present for SCC-S whereas it is not observed for conventional moldings. The shoulder at 2θ of 21.87 and d-spacing 4.064 Å is more pronounced for the SCORIM moldings and is attributable to the EVOH phase in the blend.[33] These results indicate that the EVOH forms a distinct crystalline phase in the blend, indicating a decrease of miscibility in SCORIM molded SEVA-C. Further WAXD investigations on conventionally injection-molded SEVA-C (processed over a broad processing window) did not show the presence of this peak (unpublished data).

The use of higher frequency of piston movements and higher holding pressures in SCG-S contributes to the enhancement of the crystallinity of moldings. This result is consistent with the mechanical properties increase for this set as well as with the DSC investigation presented below.

Figure 13 presents the Debye patterns gained for CM-S. The appearance of continuous Debye rings shows that almost no preferred orientation is present in the molding. Figure 14 shows the Debye pattern for SCG-S. The molecular alignment in SCORIM moldings is revealed by the Debye rings.

DSC

Figures 15 and 16 show the DSC thermograms for CM-S and SCG-S, respectively, confirming the immiscible character of the blends. Table X summarizes the DSC results for CM-S, SCC-S, and SCG-S and the respective tangent moduli. The lower melting temperature peak is for EVOH and the high melting peak is for starch. The peak area for the high melt temperature phase intensifies

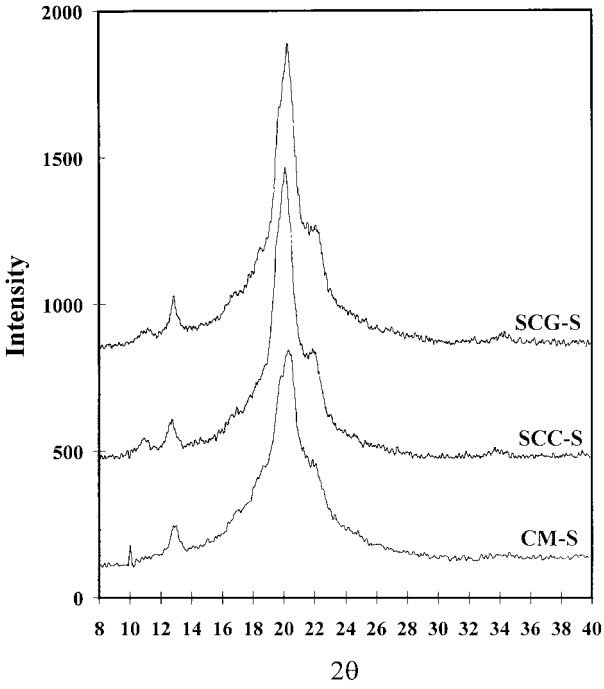

Figure 12 X-ray diffraction patterns for CM-S, SCC-S, and SCG-S moldings.

following the application of SCORIM. There appears to be a shoulder at 156°C to this peak. The total ΔH for the two peaks is greater for the

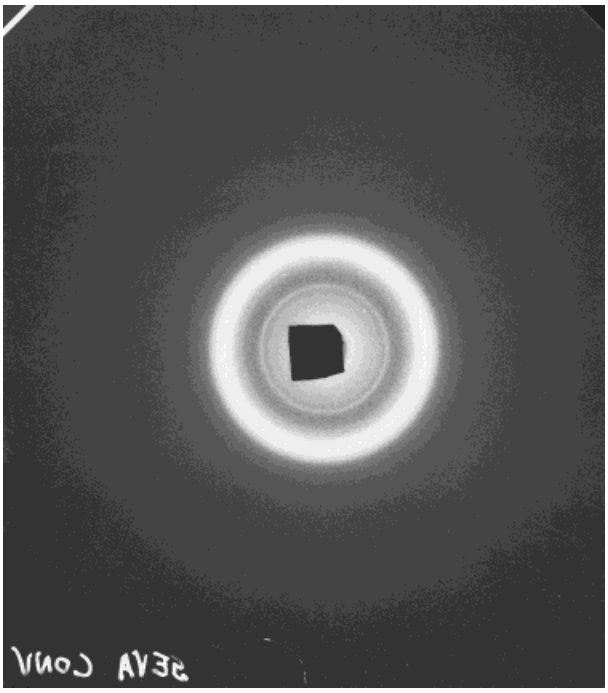

Figure 13 X-ray diffraction pattern for CM-S.

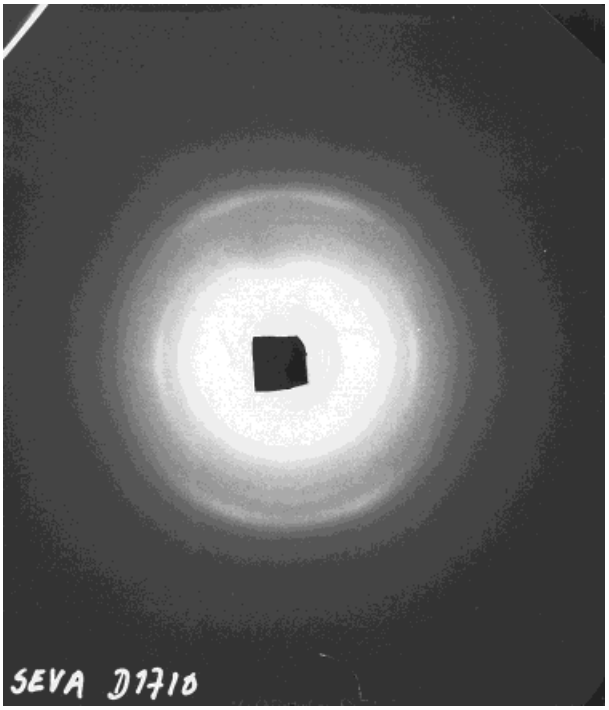

Figure 14 X-ray diffraction pattern for SCG-S.

SCORIM molded sample than for conventional moldings. This is consistent with the WAXD results presented in this article. It is worth indicating that there is a 6 to 8°C shift to lower temperatures for both peaks after the application of SCORIM, which remains to be explained.

The stiffness increment in SCORIM processed SEVA-C is attributable to the preferred orientation morphology developed as a result of the shear stress fields imposed. It was possible, by the use of the methodology proposed, to identify the critical processing parameters concerning the optimization of its mechanical properties.

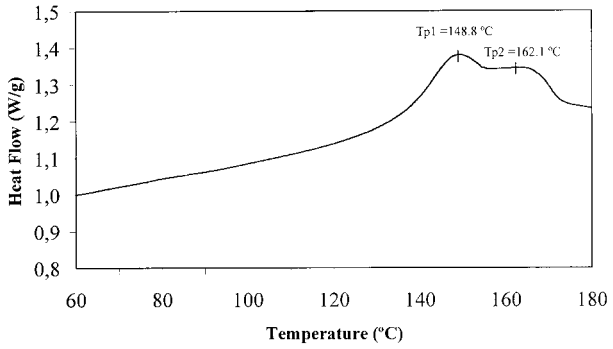

Figure 15 DSC thermogram for CM-S.

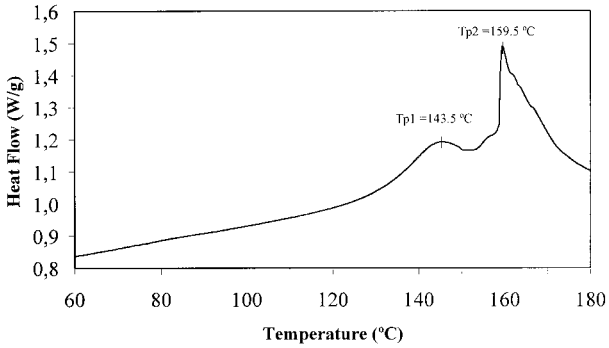

Figure 16 DSC thermogram for SCG-S.

For long durations of applied shear, stiffness depends both on holding pressure and frequency of piston movements. For DSG moldings, this dependence is correlated positively with holding pressure. However, it is also shown that a large interaction effect is present between this processing parameter and the frequency of piston movements. For the processing window analyzed, the increase of frequency of piston movements has a positive effect on stiffness for 1.3 MPa of holding pressure, whereas the opposite occurs for 2.6 MPa. This effect is also observed for the DTG moldings molded using higher levels of holding pressure. In this case the increase of frequency of piston movements was followed by a decrease of tangent modulus. These results account for optimum values of holding pressure between 4.0 and 5.0 MPa (for both DSG and DTG moldings) and frequencies of piston movements of 1.00 and 0.33 Hz respectively for DSG and DTG moldings.

By establishing processing/properties relationships it is possible to infer the importance of the processing parameters studied on the mechanical performance of the moldings and consequently on the magnitude of the shear stress fields imposed. However, the precise influence of such parameters on the shear stress field is still unknown. It is known that the viscosity of a melt depends on its

Table X DSC Results for CM-S, SCC-S, and SCG-S and the Respective Tangent Moduli

Set	T_p 1 (°C)	T_p 2 (°C)	ΔH (J/g)	Tangent Modulus (MPa)
CM-S	148.4 (0.6)	168.9 (0.5)	34.1 (0.1)	2275
SCC-S	145.3 (0.4)	159.9 (0.4)	38.8 (0.5)	2555
SCG-S	142.6 (0.4)	159.1 (0.5)	44.3 (0.3)	2972

pressure. An increase of holding pressure increases the material viscosity and consequently, for a constant shear rate, increases the shear stress (and the shear induced molecular orientation). Further increase of pressure and/or shear rate (by means respectively of holding pressure and frequency of piston movements) enhances viscous dissipation, increasing the melt temperature and consequently the amount of molecular relaxation during cooling. It is believed that the negative effect of holding pressure and frequency of piston movements on stiffness (for values above those reported as optimum) results from the increment of melt relaxation during cooling.

The pressure applied by the pistons is also an important parameter concerning the processing optimization of SEVA-C. However, its variation is not completely understood. It is supposed that piston pressures define proportionally the shear displacement of the melt, and as a consequence the shear strain, being its effect is strongly dependent on the frequency of piston movements. Optimum values of piston pressures should be proportional to the frequency of piston movements: 40 and 50% of piston pressures for respectively 0.33 Hz and 1.00 Hz of frequency of piston movements.

The stiffness increase observed in SCORIM moldings results from the extended oriented morphology induced during processing. The stiffness varies according to the crystallinity exhibited by X-ray diffraction and with the ΔH variation during melting. Although SEVA-C presents a partially crystalline structure (as shown by the scattering exhibited in the several diffraction patterns), its is worth indicating the 30% shift in ΔH during melting of SEVA-C found to occur for SCORIM moldings (SCG-S) relative to conventional molding (CM-S).

CONCLUSIONS

The conclusions of this investigation may be summarized as follows:

1. Shear controlled orientation in injection molding leads to mechanical property enhancement for starch/poly(ethylene-vinyl alcohol) blends (SEVA-C). An enhancement of 30% in tangent modulus and 20% in ultimate tensile strength was achieved with this processing method.
2. It is evident that the holding pressure and frequency of piston movements have the strongest influence on the morphological development. The influence of holding/piston pressures is very much dependent on the frequency of piston movements.
3. The solidification of SEVA-C at high cavity pressures enhances stiffness for long durations of applied shear. However, the viscous heating, and consequent thermal degradation, of SEVA-C should be considered in the adoption of processing conditions.
4. A decrease of phase miscibility in SEVA-C occurs as a result of shear controlled orientation in injection molding
5. SEVA blends exhibit preferred orientation when they are subjected to macroscopic shear during processing.

The authors acknowledge the materials kindly supplied by Novamont, Novara, Italy. The work of Rui de Sousa is financially supported by Subprograma Ciência e Tecnologia do 2° Quadro Comunitário de Apoio, Ministério da Ciência e Tecnologia (Portugal).

REFERENCES

1. Hastings, G. Composite Materials in Biomedical Engineering: Biomaterials Degradation; Barbosa, M. A., Ed.; Elsevier 1991; p. 23.
2. Soltész, U. Ceramics in Composites: Review and Current Status, Bioceramics—Material Characteristics Versus *In Vivo* Behavior; New York Academy of Sciences, Annals of the New York Academy of Sciences: New York, 1988; p. 137.
3. Bonfield, W. Bioceramics 9; Kokubo, T.; Nakamura, T.; Miyaji, F., Eds.; Elsevier Science: Oxford, 1996; p. 11.
4. Williams, D. Concise Encyclopaedia of Medical and Dental Implants; Pergamon Press: London, 1990.
5. Hayashi, T. Prog Polym Sci 1994, 19, 663.
6. Vainiopää, S. J.; Rokkanen, P.; Törmälä, P. J Polym Sci 1989, 14, 679.
7. Rokkanen, P. U. Ann Med 1991, 23, 109.
8. Litsky, A. L. J Appl Biomater 1993, 4, 109.
9. Isaac, D. H.; Green, M. Clin Mater 1994, 15, 79.
10. Ravaglioli, A.; Krajewski, A. Bioceramics: Materials, Properties, Applications; Chapman & Hall: London, 1992.
11. Knowles, J. C.; Hastings, G. W. J Mater Sci Mater Med 1992, 3, 352.
12. Knowles, J. C.; Hastings, G. W. J Mater Sci Mater Med 1993, 4, 102.
13. Reis, R. L.; Cunha, A. M. J Mater Sci Mater Med 1995, 6, 786.
14. Reis, R. L.; Cunha, A. M.; Allan, P. S.; Bevis, M. J. Polym Adv Technol 1996, 7, 784.

15. Reis, R. L.; Mendes, S. C.; Cunha, A. M.; Bevis, M. J. Polym Int 1997, 43, 347.
16. Bastioli, C.; Bellotti, V.; Del Giudice, L.; Lombi, R. PCT International Pat. Application WO91/02025, 1991.
17. Bastioli, C.; Bellotti, V.; Del Giudice, L.; Gilli, G. J Environ Polym Degrad 1993, 1, 181.
18. Allan, P. S.; Bevis, M. J. British Pat. 2170-140-B.
19. Allan, P. S.; Bevis, M. J. Plast Rubber Process Appl 1987, 7, 3.
20. Allan, P. S.; Bevis, M. J. Compos Manuf 1990, 1, 79.
21. Ogbonna, C. I.; Kalay, G.; Allan, P. S.; Bevis, M. J. J Appl Polym Sci 1995, 58, 2131.
22. Kalay, G.; Zhong, Z.; Allan, P. S.; Bevis, M. J. Polymer 1996, 37, 2077.
23. Kalay, G.; Bevis, M. J. J Polym Sci Part B Polym Phys 1997, 35, 241.
24. Kalay, G.; Bevis, M. J. J Polym Sci Part B Polym Phys 1997, 35, 265.
25. Kalay, G.; Allan, P. S.; Bevis, M. J. Kunstsoffe 1997, 87, 6, 768.
26. Kalay, G.; Bevis, M. J. J Polym Sci Polym Phys 1997, 35, 415.
27. Reis, R. L.; Cunha, A. M.; Allan, P. S.; Bevis, M. J. Adv Polym Technol 1997, 4, 276.
28. Reis, R. L.; Cunha, A. M.; Bevis, M. J. Med Plast Biomater 1997, 6, 46.
29. Reis, R. L.; Cunha, A. M.; Bevis, M. J. Antec'98—Plastics on My Mind; Soc. Plastics Eng., Atlanta, GA, April/May, 1998.
30. Ross, J. P. Taguchi Techniques for Quality Engineering; McGraw Hill: New York, 1998.
31. Schmidt, S. R.; Launsby, R. G. Understanding Industrial Designed Experiments, 4th ed.; Air Academy Press: Colorado, 1994.
32. Montgomery, D. C. Design and Analysis of Experiments, 3rd ed.; Wiley: New York, 1991.
33. Simmons, S.; Thomas, E. J Appl Polym Sci 1995, 58, 2259.